ARMA/NARMS 04-512

SEISMIC MONTINORING OF FRACTURE ALTERATION BY MINERAL DEPOSITION

Zane Gilbert
Department of Physics, Purdue University, West Lafayette, Indiana, USA

Laura J. Pyrak-Nolte
Department of Physics, Purdue University, West Lafayette, Indiana, USA

Department of Earth and Atmospheric Sciences, Purdue University, West Lafayette, Indiana, USA

This paper was prepared for presentation at Gulf Rocks 2004, the 6th North America Rock Mechanics Symposium (NARMS): Rock Mechanics Across Borders and Disciplines, held in Houston, Texas, June 5 – 9, 2004.

ABSTRACT: Fluid flow and compressional wave propagation measurements were made on fractured samples prior to and after the chemical deposition of calcium carbonate. We observed that the initial void geometry (aperture and contact area) controlled the amount and spatial distribution of mineral deposition within the fracture. The most reliable seismic indicator that the fracture had been altered is a reduction in the width of the distribution of the most probable frequency in the received signal. A reduction in the width of the distribution indicates that the fracture is homogenized by mineral deposition in the fracture voids. Homogenization occurs because the mixing predominantly takes place in the dominant flow paths within the fracture which tend to have low fracture stiffness. The results indicate that acoustic imaging techniques are required in this characterization because they provide a statistical indicator to monitor changes in fracture geometry caused by mineral deposition.

1. INTRODUCTION

The construction of underground structures can alter the underground environment by changing the local stress distribution as well as the local hydrogeology of a site. Depending on the purpose of the underground structure, long-term monitoring of underground environments may be required because fractures, joints and faults can be altered over the lifetime of the engineered structure. Because rocks are part of the tectonic and hydrogeologic cycles, the geometry of the voids and contact area in a fracture can be altered by time-dependent processes such as normal and shear displacement, weathering, chemical precipitation, and chemical dissolution. For example, CO_2 injection into a subsurface reservoir can initiate a complex set of reactions that involves interactions between aqueous solutions and the minerals in the host rock. CO_2 can transfer across a gas-water interface to become an aqueous ion by the reaction:

$$CO_2\,(g) + H_2O = H_2CO_3$$

This is followed by rapid dissociation of carbonic acid:

$$H_2CO_3 = H^+ + HCO_3^-$$

The formation of bicarbonate ion, HCO_3^-, and production of acidity by release of H^+ leads to a series of secondary reactions. These reactions complicate estimates of CO_2 storage volumes as well as measurements of the geophysical characteristics of the rock. If minerals precipitate in a fracture or if the fracture void geometry is dissolved because of CO_2 injection, the geometrical properties of the fracture will change and may alter the hydraulic and seismic properties of the fracture. In this study, we used acoustic measurements to monitor the deposition of calcium carbonate in a fracture and its effect on hydraulic properties of single fractures.

2. EXPERIMENTAL METHOD

2.1. Sample Preparation

Granitic samples were used to study wave propagation across a fracture prior to and after mineral precipitation within a fracture. The samples were made from Barre granite which had no connected matrix porosity. The compressional wave velocity for an intact sample (i.e., no through-going fractures) was 3520 m/s and the shear wave velocity was 2570 m/s. An intact ample, GI04, was used for control experiments. Four fracture samples, GF01, GF03, GF05 and GF08, were created for this investigation by inducing a single fracture in each using a technique similar to brazil testing [1]. Samples GF03 and GF05 were acoustically characterized prior to inducing the fracture. The samples were approximately 110 mm x 104 mm x 70 mm. Acoustic measurements were made across the 70 mm dimension with the fracture located approximately halfway. After inducing the fracture, eight flow ports (Fig. 1) were attached to the sample and the remaining exterior portions of the fracture were sealed with marine putty. Samples GF01 and GF03 were subjected to no load while samples GF05 and GF08 were held in an aluminum frame to apply a small load to the sample. Tygon tubing was attached to each port.

2.2. *Hydraulic Measurements and Chemical Invasion*

Figure 1 is a sketch of the location of the flow ports. A falling head method was used to measure the volumetric flow rate through the sample prior to chemical invasion in the fracture. One month after chemical invasion, the fracture was re-saturated with water and volumetric flow rates were re-measured.

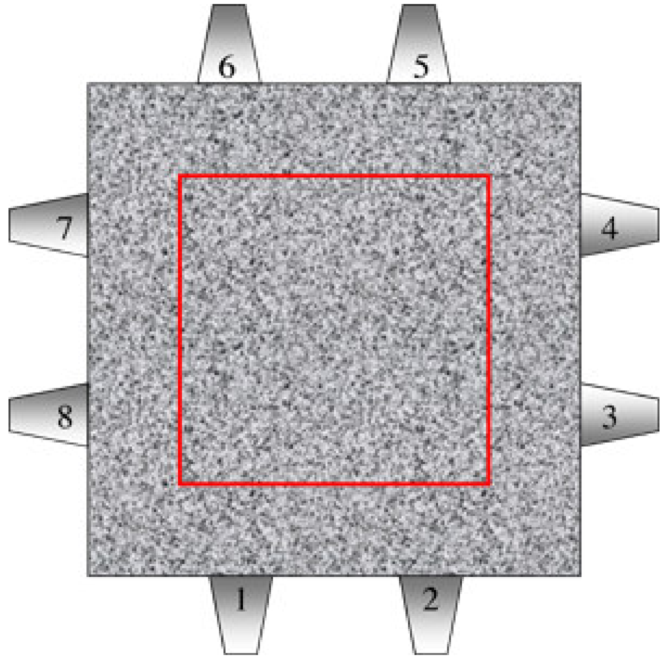

Fig. 1. Sketch of sample and location of ports (1-8) for fluid flow measurements and chemical invasion. The area that was seismically squared is shown by the square.

A chemical invasion method was used to induce mineral precipitation within the fracture. In this method, two chemicals were invaded into the fracture through two separate flow ports (ports 1 and 2 in Fig. 1) which upon combination cause the precipitation of calcium carbonate, $CaCO_3$. The two chemical solutions that were used to precipitate calcium carbonate are Calcium Acetate Hydrate ($Ca(CH_3COO)_2$ * H_2O), and Sodium Hydrogen Carbonate ($NaHCO_3$). These two chemicals were applied in concentrations of 0.1M in a 1:1 ratio. During the chemical invasion, ports 3 through 8 were left open. For all chemically invaded samples, the invasion period was approximately two hours.

2.3. *Acoustic Measurements*

To measure the seismic properties of a fracture undergoing mineral precipitation, we use an acoustic imaging method [2-4]. This technique is capable of acquiring the full arriving waveform in two spatial dimensions and one temporal dimension. From this three-dimensional dataset, we reconstruct the longitudinal components of acoustic waves that have propagated through a sample, and thereby obtain a direct visualization of heterogeneity within the sample caused by mineral precipitation.

To perform acoustic measurements, a sealed water-saturated fracture sample is placed in a water tank. Two plane-wave, water-coupled, broadband, piezoelectric transducers with a central frequency of 1 MHz (or central wavelength of approximately 3.5 mm) are used to send and receive compressional waves. Water-coupled transducers are used to provide uniform coupling between the transducers and the sample for all locations on the sample. Transmitted compressional waves were recorded in 1 mm increments within a 64 mm by 64 mm region of the sample to determine the spatial variation in fracture properties before and after the precipitation of calcium carbonate in the fracture. This results in the acquisition of 4096 signals per dataset. Figure 1 shows the location of the scanned area relative to the size of the sample. The translation of the source and receiving transducers is performed using computer-controlled linear actuators (Newport 850-B4 with Newport Motion Master 2000). A pulse generator (Panametrics PR1500) was used to pulse the sending transducer and receive the transmitted compressional wave. The received waveforms were amplified. At each receiving location, 5000 points of the waveform are recorded, which represents a 50 microsecond window containing the compressional-wave and other arrivals. The received waveforms were digitized (Lecroy 9314L) and stored on a computer for analysis. Because acoustic measurements were performed over a period of a month, reflection times were used to insure that the source and receiver were always placed the same distance away from the sample.

3. EXPERIMENTAL RESULTS AND ANALYSIS

3.1. Received Acoustic Waveforms

Prior to and after chemical invasion, the water-saturated fracture samples were acoustically characterized. Figures 2 & 3 show a 10 microsecond window of the received compressional-waves for samples GF01 and GF05, respectively, from the center of the sample. For sample GF01, the compressional wave amplitude initially decreased because of the generation of gas (CO_2) from the chemical reaction. After 15 days, the signal amplitude from sample GF01 increased three-fold as a result of the deposition of minerals in the fracture. Sample GF05, which was under a small load, also exhibited an increase in the transmitted wave amplitude after chemical invasion. The signals from sample GF05 also indicate that the frequency content of the signal is altered by mineral precipitation. The period of one-cycle of the waveform is observed to decrease indicating a higher frequency content.

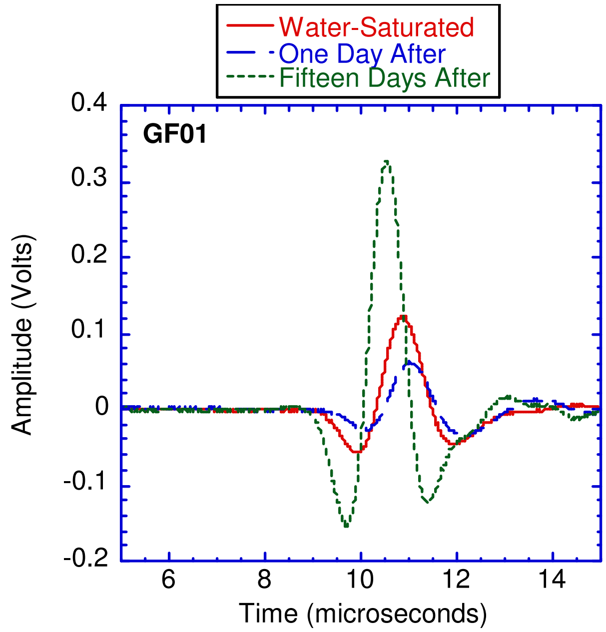

Fig. 2. Received compressional waveforms for fractured sample GF01 in the water-saturated condition, one-day after mineral precipitation and fifteen days after mineral precipitation.

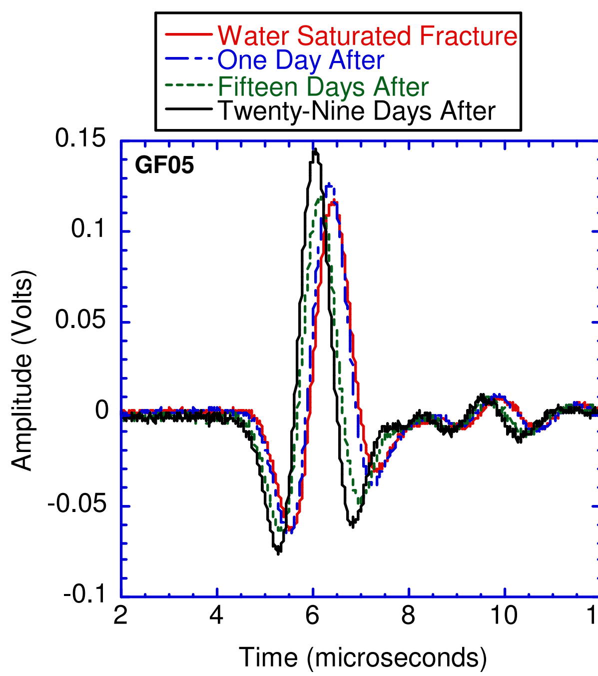

Fig. 3. Received compressional waveforms for fractured sample GF05 in the water-saturated condition, one-day after

mineral precipitation, fifteen days after mineral precipitation. And twenty-nine days after mineral precipitation

3.2. Waveform Analysis

To examine the frequency content of the signal, a wavelet analysis was performed on the received compressional waves. For this analysis, a Hilbert wavelet method [5] was used that provides equal accuracy in time and frequency. The wavelet analysis produces a two-dimensional transform that quantifies how the frequency content of the signal changes with time. In the wavelet transformation, the spectra, the dominant amplitude and the most probable frequency are used for comparing changes in the signal as a function of days after chemical invasion. The most probable frequency is the frequency at which the maximum in amplitude (i.e., dominant amplitude) occurs.

Figures 4 & 5 show the spectra from wavelet analysis of the compressional wave signals for samples GF01 and GF05 in the water-saturated condition and after chemical invasion for signals taken from the center of the scanned region. For both samples in the water-saturated condition, the most probable frequency is 0.5 MHz. For sample GF01, the signal amplitude reached a minimum 95 minutes after chemical invasion and started to increase after that time. By 15 days after chemical precipitation, the most probable frequency of the signal for sample GF01 increased to 0.6 MHz. The

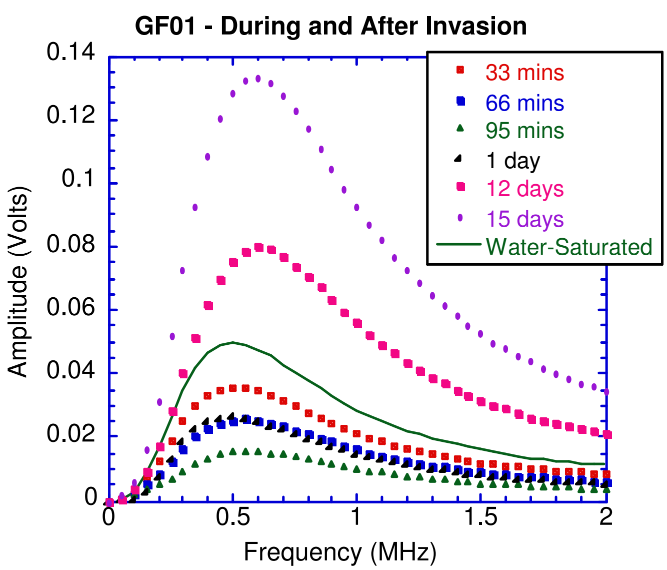

Fig. 4. Spectral content of received waveforms for fractured sample GF01 in the water-saturated condition prior to chemical invasion and for 33 min., 66 min., 95 min., 1 day, 12 days and 15 days after chemical invasion.

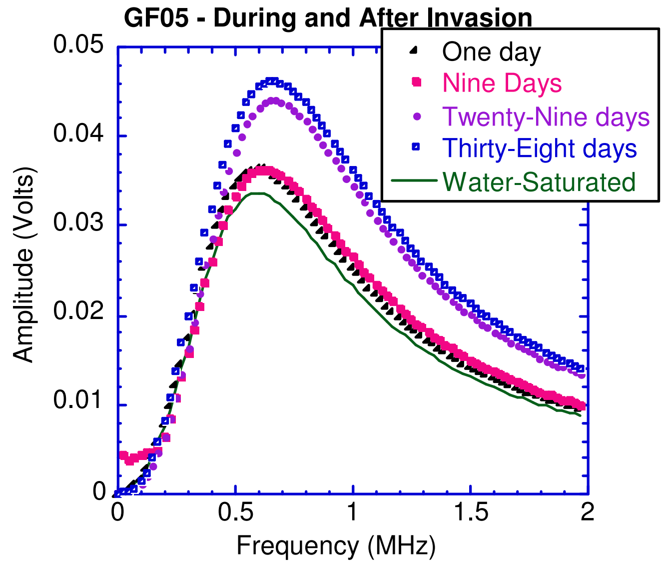

Fig. 5. Spectral content of received waveforms for fractured sample GF05 in the water-saturated condition prior to chemical invasion and for 1 day, 9 days, 29 days and 38 days after chemical invasion.

signals from sample GF05 also exhibited the same shift in the most probable frequency but had lower amplitudes than samples GF01.

3.3. Acoustic Images of the Fracture Samples

In this section, we present two-dimensional images of the acoustic response of a fracture undergoing mineral precipitation. It was hypothesized that the flow path geometry in the fracture would control the amount of mixing of the two chemical solutions within the fracture, and in turn control where mineral precipitation occurred.

Figure 6(a-c) shows the dominant seismic amplitude obtained from wavelet analysis of each signal for the sampled region (62 mm by 62 mm) for sample GF03. For the water-saturated condition (Figure 6a), the amplitudes are relatively uniform except for a region of low amplitude represented by white in the image. After chemical invasion, the dominant seismic amplitude increased with time (Figure 6b&c). Comparing Figures 6a to Figures 6b&c, it appears that chemical invasion altered the fracture through mineral deposition. Regions of the fractures that initially exhibited low amplitudes show an increase in amplitude relative to other regions of the fractures.

The relative amplitude (i.e., the post invasion amplitude (Fig 6c) minus the pre-invasion amplitude (Fig 6a), divided by the pre-invasion amplitude (Fig 6a)) is shown in Figure 6d. From the relative amplitude (Figure 6d), the amplitudes increased in some regions as much as 4700%. The largest relative change in amplitude occurred in regions of the fracture that originally (Figure 6a - white regions) exhibited low amplitudes (i.e., low fracture stiffness and hence large aperture) [6,7]. It is hypothesized that much of the flow and chemical interaction occurs in the largest fracture apertures which would initially exhibit low seismic amplitude. If most of the flow occurs in the largest apertures, the change in fracture specific stiffness can be caused by aperture reduction from mineral deposition and also by stiffening of the contact regions.

3.4. Frequency Content of Signals

The wavelet analysis provides data on the most probable frequency of the arriving energy. Figure 7 is a histogram of the most probable frequency (based on 4096 analyzed signals) for a control-sample GF08 which contained a single-induced fracture but was not subjected to chemical invasion in the first 41 days. Figure 8 is a histogram of the most probable frequency for the fractured sample GF03 in the water-saturated condition, and the

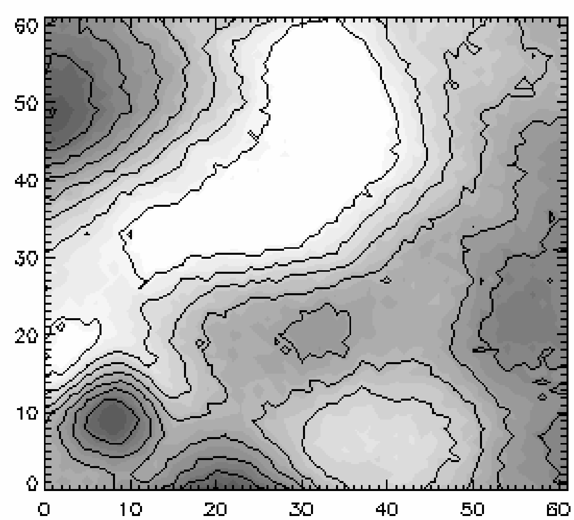

Fig. 6a. Acoustic image of the transmitted amplitude for sample GF03 in the water-saturated condition. The color bar is given Fig. 6e.

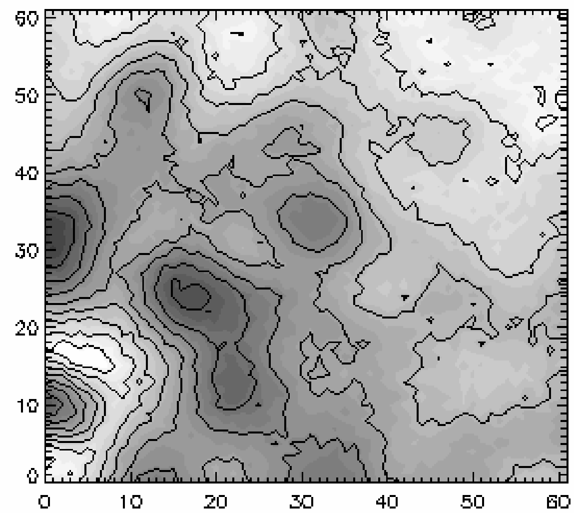

Fig. 6c Acoustic image of the transmitted amplitude for sample GF03 thirty-two days after chemical invasion and resaturation with water. The color bar is given Fig. 6e.

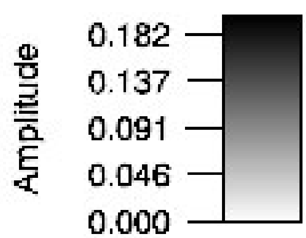

Fig. 6e. Color scale for Figures 6a, 6b and 6c.

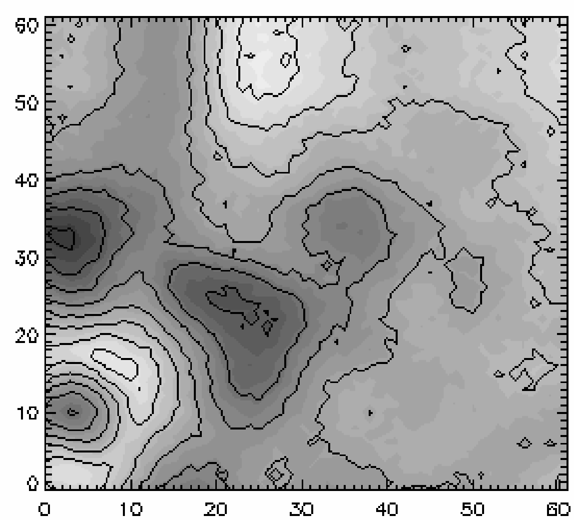

Fig. 6b. Acoustic image of the transmitted amplitude for sample GF03 seven days after chemical invasion. The color bar is given Fig. 6e.

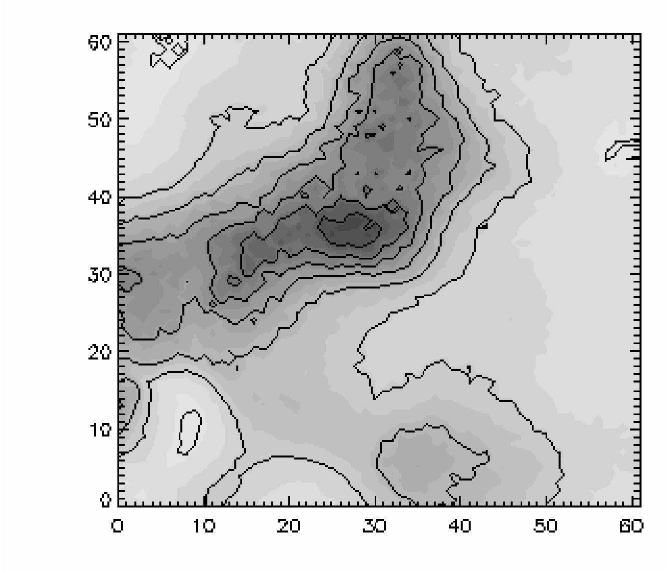

Fig. 6d. Acoustic image of the relative amplitude for sample GF03. The color bar is given Fig. 6f. The color scale is in Fig. 6f.

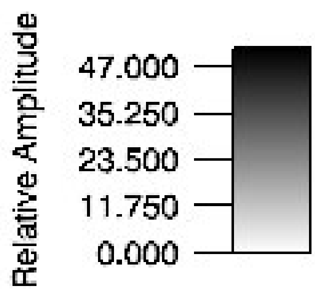

Fig. 6f. Color scale for relative amplitude for Figure 6d on the right.

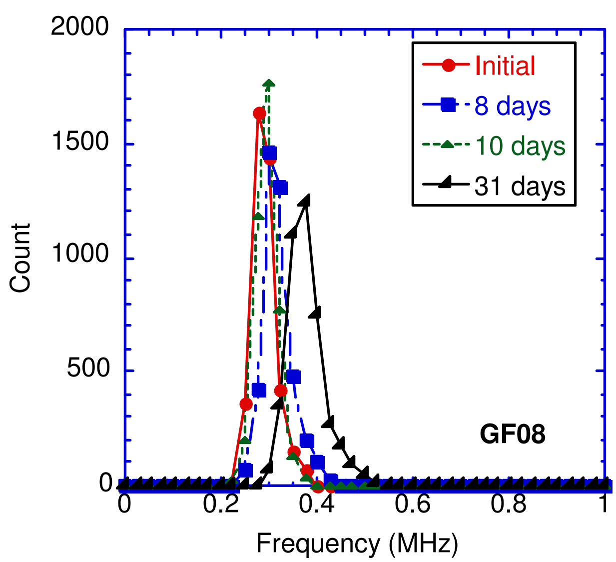

Figure 7. Histogram of the most probable frequency for sample GF08.

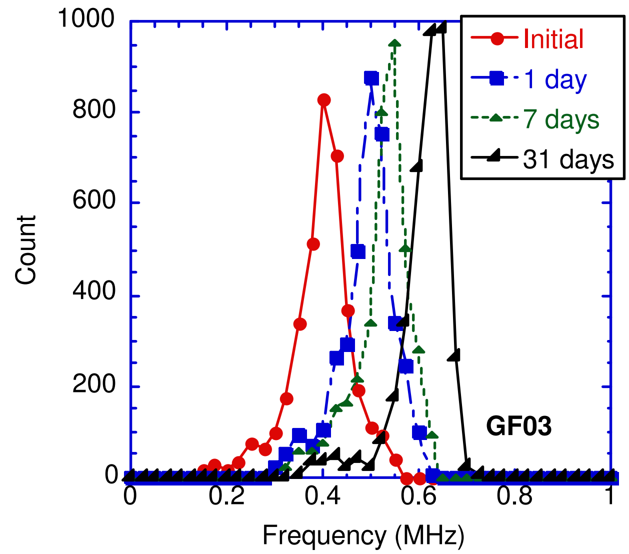

Figure 8. Histogram of the most probable frequency for sample GF03.

fracture after chemical invasion, based on all the signals collected in the 64 mm by 64 mm region. With and without mineral precipitation, the most probable frequency shifted to higher frequency over time. However, for sample GF03 (Fig. 8) which was subjected to chemical invasion, the width of the histogram is observed to decrease after chemical invasion, while the histogram for sample GF08 (Fig. 7) exhibited a broadening of the distribution (increase in width). The decrease in width of the histograms for fractured samples subjected to chemical invasion indicate that mineral precipitation in the fracture is homogenizing the fracture, i.e., low stiffness regions of the fracture are stiffening more than originally high stiffness regions. This is consistent with the acoustic imaging results for sample GF03 shown in Figures 6. For example, the acoustic map of relative amplitude (Figure 6d) shows that the largest changes in transmitted amplitude for sample GF03 occurred in the region that originally (Figure 6a) had the lowest amplitude.

Fig. 9 is a graph of the root variance in the width of the histogram of the dominant frequency for fractured samples GF03, GF05 and GF08 and for an intact control-sample GI04. Sample GI04 was never fractured or subjected to chemical invasion. However, the width of the frequency distribution for intact control sample GI04 was observed to increase over time. Fracture control sample GF08 contained a single-induced fracture and was not subjected to chemical invasion until 42 days after the initial water-saturation. In Fig 9., an increase in the width of the frequency distribution for GF08 is observed up to 41 days. The increase in the width of the distributions for control samples GI04 and GF08 (prior to day 42) is hypothesized to be a result of surface chemistry occurring on the samples. All of the samples are maintained in a water-tank throughout the acoustic imaging measurements. The samples are not moved between measurements which insure that the same location is imaged over time.

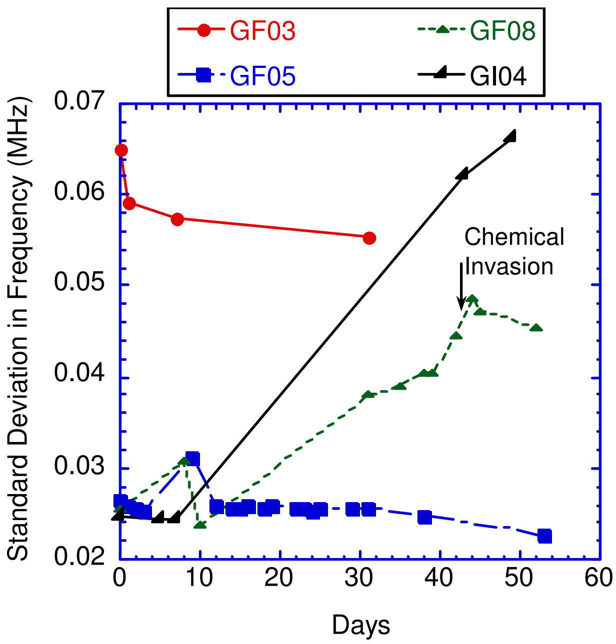

Fig. 9. The change on the root variance (standard deviation or width) of the frequency distributions for samples GF03, GF05, GF08 and GI04 as a function of time.

The samples subjected to chemical invasion (GF03 and GF05) exhibit a decrease in the width of the frequency distribution. A reduction in the width of the frequency histogram indicates that fracture specific stiffness is homogenizing over the fracture plane. This is also observed for sample GF08 after chemical invasion. After chemical invasion on the 41st day (arrow in Fig. 9), the fracture in sample GF08 began to homogenize and the width of the distribution began to decrease.

3.5. Volumetric Flow Rates

Volumetric flow rates were measured for the fracture samples prior to and approximately one month after chemical invasion. Figures 10 and 11 show the pre-invasion (before chemistry) and post-invasion (after chemistry) average flow rates for samples GF03, GF05 and sample GF08. Figure 10 contains the average flow rate for the vertical direction for measurements made between ports 1 & 5, 1 & 6, 2 & 5 and 2 & 6 (first number is the inlet, the second number is the outlet and all other ports are closed, port numbers are shown in Fig. 1). Figure 11 shows the average horizontal flow rates which are based on flow measurements made between ports 3 & 7, 3 & 8, 4 & 7 and 4 & 8. The average flow rates are graphed as a function of the root variance of the frequency distribution (standard deviation or width of the distribution). Sample GF03 and GF05 exhibited a decrease in flow rate and a decrease in the width of the frequency distribution. The decrease in flow rate can be attributed to reduction of the fracture aperture and blocking of flow paths by mineralization. While the decrease in the standard deviation indicates that mineral precipitation homogenized the fracture plane (i.e. tending toward a move uniform fracture stiffness).

Control sample GF08 was subjected to chemical invasion 41 days after initial saturation with water. Prior to chemical invasion, the standard deviation in the frequency distribution increased (Fig. 9). Thus, relative to day 40 in Fig. 9, the width of the distribution is larger for time later than day 40. However, after chemical invasion the width of the distribution decreased (Fig. 9).

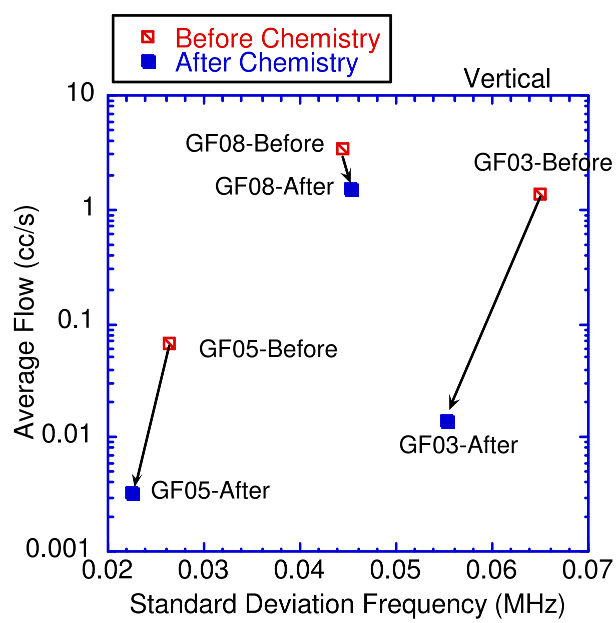

Fig. 10. Average flow rate (in the vertical direction) as a function of change in the width of the frequency distribution for samples GF03, GF05 and GF08.

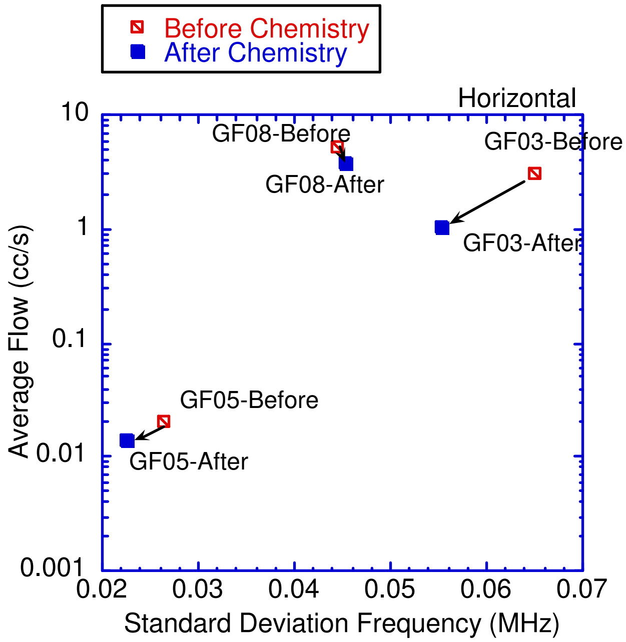

Fig. 11. Average flow rate (in the horizontal direction) as a function of change in the width of the frequency distribution for samples GF03, GF05 and GF08.

The change in flow rate from prior to chemical invasion to after chemical invasion indicates that the initial fracture void geometry controls mineral deposition within the fracture. In these experiments, the mixing of the two fluids induces precipitation of calcium carbonate. If the fracture apertures are large, the precipitate will flow through the sample and out of the ports leaving very little mineral deposition in the fracture. This occurred for sample GF08 which supported the most flow but exhibited the smallest change in flow rate after mineral deposition. If the fracture apertures are small, the volume of chemicals introduced into the fracture during the invasion period is less than for larger aperture fractures and the ability to mix is reduced. Sample GF05 had the smallest apertures as indicated by the smallest value of before chemistry flow (Figs 10 & 11). The rate of mixing and equilibration also takes longer because of the small apertures. Sample GF03 exhibited the largest change in the standard deviation of the frequency distribution and had a flow rate intermediate to samples GF05 and GF08. From the relative acoustic amplitude images (Fig. 6d) of sample GF03, it is observed that most of the mineral deposition occurred in the dominant flow path. This is also indicated by the large decrease in the flow rate for both the vertical (Fig. 10) and horizontal (Fig. 11) directions.

4. CONCLUSIONS

For mineral precipitation from the mixing of two fluids, the initial fracture void geometry controls the amount, the time-rate of mixing and the spatial distribution of mineral deposition within the fracture. If the fracture apertures are large, the precipitates flow out of the sample and leave very little mineral deposition within the fracture. If the fracture has very small apertures, the volume mixing of the two chemicals is reduced and the time-rate of mixing is long. Thus, the fracture void geometry determines mineral deposition when mineral precipitation is the result of mixing of two fluids. Other factors may dominate if mineral deposition is the result of a single fluid cooling over time.

The most reliable seismic indicator that mineral deposition occurred within the fracture was a narrowing of the width of the distribution of the most probable frequency. The narrowing of the distribution indicates that mineral deposition in the fracture is homogenizing the fracture stiffness. Regions of the fracture that initially exhibited high attenuation of the acoustic signal showed the largest increase in transmission after mineral deposition. Because mineral deposition mainly occurs in the dominant flow paths (i.e. large apertures - low stiff), those region stiffen either by a reduction in aperture or an increase in contact because the of the mineral deposition. If the background effects observed in the control sample were removed, the change in width of the frequency distribution would likely be larger.

A change in the width of a distribution is a statistical indicator and therefore requires imaging (i.e., many signals). From sampling theory, the same statistically significant results would be obtained if only 256 data points out of 4096 had been used. Because mineral deposition does not occur uniformly, a single point measurement cannot be used to monitor changes in the fracture caused by mineral deposition when the matrix of the rock is also being altered. Quantification of heterogeneity requires imaging in order to capture fracture complexity and multiple length scales.

ACKNOWLEDGMENTS: The authors wish to acknowledge support of this work by the by the Geosciences Research Program, Office of Basic Energy Sciences US Department of Energy (DE-

FG02-97ER14785 A4) and Purdue University - University Faculty Scholar.

REFERENCES

1. Jaeger, J. C.. and N. G. W. Cook. 1969. *Fundamentals of Rock Mechanics*. Methuen & Co. LTD. London.
2. Hauser, M. R., Weaver, R. L. and J. P. Wolfe. 1992. "Internal diffraction of ultrasound in crystals: Phonon focusing at long wavelengths." Phys. Rev. Lett. 68: 2605-2607.
3. Nagy, P. B., Bonner, B. P., and L. Adler. 1995. Slow wave imaging of permeable rocks. Geophys. Res. Lett. 22(9): 1053-1056.
4. Pyrak-Nolte, L. J., Mullenbach, B. L., and S. Roy. 1996. Interface waves along fractures, Journal of Applied Geophysics. 35:79-87.
5. Nolte, D. D., Pyrak-Nolte, L. J., Ziegler, C., and J. Beachy,. 2000. Transition from the displacement discontinuity limit to the resonant scattering regime for fracture interface waves, International Journal of Rock Mechanics, Mining Science & Geomechanics Abstracts. 37:245-262.
6. Pyrak-Nolte, L. J., Myer, L.R. and N.G.W. Cook,. 1990. Transmission of seismic waves across single natural fractures, J. Geophys. Res. 95(B6):8617-8638.
7. Pyrak-Nolte, L. J. and J. P. Morris. 2000. Single fractures under normal stress: The relation between fracture specific stiffness and fluid flow, International Journal of Rock Mechanics Mining Science & Geomechanics Abstracts. 37:245-262.